ORIGINAL ARTICLE
UDC 531
https://doi.org/10.26907/2541-7746.2025.4.675-688

Numerical analysis of the dynamic response of a structure equipped with friction pendulum bearings

T. Zhelyazov

National Institute of Geophysics, Geodesy and Geography (NIGGG), Bulgarian Academy of Sciences, Sofia, Bulgaria

elovar@yahoo.com

Abstract

This article focuses on the implementation of a lightweight model of a friction pendulum bearing in the finite-element model of a base-isolated structure. The proposed approach appears as an alternative to a high-fidelity finite-element model. The model considers the slider moving on the sliding surface as a material point with three degrees of freedom. The equations of motion for the slider are derived by leveraging the Lagrangian formalism. The three-degrees-of-freedom model is compared with other available analytical approaches that can be employed to define the response of friction pendulum bearings, mainly unidirectional formulations. From the numerical experiments, the dynamic response of a structure with and without base isolation is obtained using a finite-element analysis. Acceleration time series, recorded during an earthquake, are employed as an input. The numerical results, in terms of displacement and acceleration evolutions, demonstrate the positive effect of seismic isolation on mitigating the risk of failure in the structure.

Keywords: base-isolated structure, friction pendulum bearing, analytical model, finite-element modeling, transient analysis

For citation: Zhelyazov T. Numerical analysis of the dynamic response of a structure equipped with friction pendulum bearings. *Uchenye Zapiski Kazanskogo Universiteta. Seriya Fiziko-Matematicheskie Nauki*, 2025, vol. 167, no. 4, pp. 675–688. https://doi.org/10.26907/2541-7746.2025.4.675-688.

ОРИГИНАЛЬНАЯ СТАТЬЯ
УДК 531
https://doi.org/10.26907/2541-7746.2025.4.675-688

Численное исследование динамической реакции конструкции с фрикционно-маятниковыми опорами

Т. Желязов

Национальный институт геофизики, геодезии и географии (НИГГГ),
Болгарская академия наук, г. София, Болгария

elovar@yahoo.com

Аннотация

Разработана упрощенная модель фрикционно-маятниковой опоры, применяемой при конечно-элементном расчете конструкции с сейсмоизолированным фундаментом. Упрощенная модель выступает в качестве альтернативы детализированной конечно-элементной модели опоры и описывает движение, совершаемое ползуном, представленным в виде материальной точки с тремя степенями свободы, по поверхности скольжения. Уравнения движения ползуна получены с использованием формализма Лагранжа. Проведено сравнение данной модели с известными аналитическими моделями, прогнозирующими поведение фрикционно-маятниковых опор, преимущественно однонаправленных. Динамическое поведение сейсмоизолированной конструкции и её варианта при отсутствии сейсмоизоляции изучено посредством численных экспериментов с помощью метода конечных элементов. В качестве входных данных использовались акселерограммы, записанные во время землетрясения. Анализ численных данных, характеризующих амплитуду перемещения и ускорения сейсмоизолированной конструкции, показал, что применение сейсмоизоляции значительно снижает риск повреждения конструкций.

Ключевые слова: строительная конструкция с сейсмоизоляцией, фрикционно-маятниковая опора, аналитическая модель, конечно-элементное моделирование, анализ переходных процессов

Для цитирования: *Zhelyazov T.* Numerical analysis of the dynamic response of a structure equipped with friction pendulum bearings // Учен. зап. Казан. ун-та. Сер. Физ.-матем. науки. 2025. Т. 167, кн. 4. С. 675–688. https://doi.org/10.26907/2541-7746.2025.4.675-688.

Introduction

Seismic isolation decouples the structure from the ground by providing lateral flexibility, while ensuring sufficient rigidity to withstand vertical loads transmitted from the superstructure [1, 2]. Base isolation serves as an efficient method to reduce displacements in the superstructure during a strong ground motion by dissipating the energy from seismic waves. This goal is achieved by adding friction or flexibility. The most common examples of dissipative devices are friction pendulum systems [3], high damping rubber bearings, and lead core rubber bearings (LRB) [4].

Typically, a friction pendulum isolator consists of top and bottom steel plates and a steel slider. The bottom steel plate is machined to form a concave sliding surface on which the slider moves. The surfaces of the slider, which are in contact with other elements of the bearing, may be covered with a composite material liner to obtain some desired characteristics of the sliding behavior (Fig. 1).

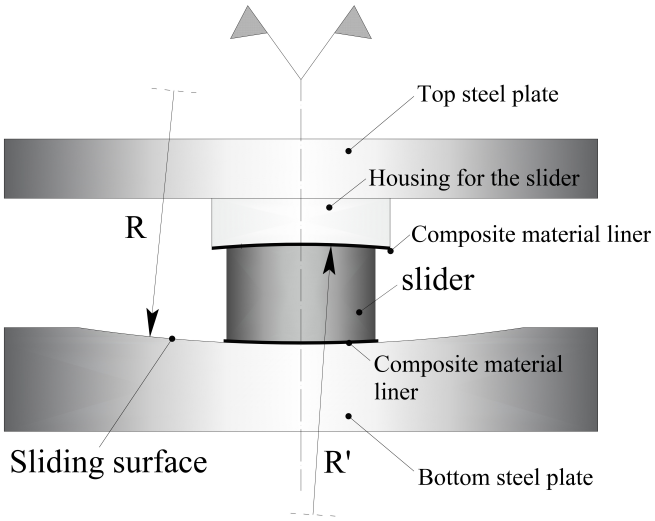

Fig. 1. Friction pendulum isolator

The sliding surface is characterized by little resistance to lateral movement due to the low coefficient of friction. Therefore, the device has a large capacity for movement, which is limited only by its geometric dimensions in the plane.

Friction isolators have garnered substantial research interest [5–8]. The period of oscillation of a structure equipped with friction pendulums depends mainly on the radius of curvature of the concave sliding surface rather than on the supported mass [7]. Friction isolators are generally compact, making them an attractive option for retrofitting existing buildings [8]. They have proven effective for seismic isolation of certain types of structures [9,10] and bridges [11] as well.

Some technological demands, such as the need to limit displacement of the sliding isolator during a strong ground motion, have led to the development of triple [12,13] and quintuple [14] friction isolators that accommodate more sliding surfaces and provide multiple regimes of response during a seismic excitation. Furthermore, friction pendulum bearings with variable curvature were proposed and studied [15–19]. The variable curvature of the sliding surface theoretically enables an adaptive frequency conversion, thus minimizing the likelihood of undesired effects associated with resonance. In contrast, classical friction pendulum bearings provide a constant isolation frequency, which is associated with a higher risk for resonance occurrence. Apart from being an option for base isolation, friction pendulum bearings emerge as a solution for inter-story seismic isolation. High-rise buildings equipped with inter-story isolation reportedly demonstrate a better response compared to those with base isolation [20].

Dynamic structural behavior analysis has always been a challenge, given that no straightforward recipe exists. Finite-element analysis of a base-isolated structure can provide some insight into the response during an earthquake without restriction regarding possible irregular geometry. In terms of seismic isolation modeling, several approaches are possible. One solution is to develop a high-fidelity finite-element model of the bearing, which will

add a considerable number of degrees of freedom to the finite-element model of the base-isolated structure that might be comparable to the degrees of freedom of the structure. This approach will clearly result in an increased overhead in terms of computational resources and time for analysis. The question arises of how to implement less demanding models to reduce the computational load in the transient finite-element analysis of the entire structure.

Existing analytical models have evolved from single-degree-of-freedom (SDOF) approximations, capable of capturing the response of friction seismic isolators with acceptable accuracy, to a vector superposition of two, inherently SDOF responses, along two orthogonal directions assumed independent of each other [21, 22].

The need to go beyond SDOF approaches and take into account the multiaxial response of friction pendulum bearings was suggested by indicating that the bearing response depends on the supported vertical load [23,24]. In more recent studies [25], it was argued that models rooted in SDOF approximations neglect some phenomenological aspects of the friction pendulum response, which might be important in the case of near-fault ground motions characterized by a better pronounced vertical component. In one of the proposed models, the motion of the slider on the spherical concave surface is considered as the motion of a particle with three degrees of freedom.

Machine learning algorithms also find application in analyzing the dynamic response of structures, as well as in reproducing the behavior of seismic isolation. The relative displacement of stories was investigated in [26]. A hybrid analysis comprising modeling of the superstructure using linear frame models and ANN implementation for the force-displacement relationship of the seismic isolators was presented in [27] and validated in [28] via a comparison with conventional time history analysis and test data. It should be noted that this analysis was conducted for another type of isolator, not for friction pendulum bearings.

The scope of the contribution is confined to the application of approaches rooted in analytical mechanics combined with time-history analysis using finite-element models for structures with base isolation in classical friction-pendulum bearings (Fig. 1).

The article is organized as follows. The SDOF model application is illustrated through the numerical simulation of a friction pendulum bearing characterization test. The force-displacement relationships in two orthogonal directions are numerically obtained. The analytical approach in which the motion of the slider is considered a motion of a material point with three degrees of freedom is then introduced. Finally, the behavior of a base-isolated structure, in which the three-degrees-of-freedom model of the device is implemented, during an earthquake is analyzed using a transient finite-element analysis. The response of the structure is obtained in terms of displacements and accelerations. To underscore the effect of the seismic isolation, the responses of two identical structures with and without base isolation are compared.

1. Combination of One-Dimensional Models in Two Orthogonal Directions

In this section, an approach assuming a combination of two SDOF models in two orthogonal directions is considered. The analytical model is implemented to numerically evaluate the behavior of a friction pendulum bearing subjected to in-plane excitation and a vertical load. In the sequel, the numerically obtained relationships are referred to as U-F relationships.

$$\begin{pmatrix} F_x \\ F_y \end{pmatrix} = \frac{\mathbf{N}}{r} \begin{pmatrix} u_x \\ u_y \end{pmatrix} + \mu \mathbf{N} \frac{1}{\|\dot{u}\|} \begin{pmatrix} \dot{u}_x \\ \dot{u}_y \end{pmatrix}, \tag{1}$$

where $\mathbf{N}$ is the vertical load transferred from the superstructure, r is the effective radius of the sliding surface $\mathbf{u} = (u_x, u_y)^T$, $\dot{\mathbf{u}} = (\dot{u_x}, \dot{u_y})^T$, and T denotes a transpose.

The model defined by equation (1) can be implemented in the characterization test shown in Fig. 2. The bottom plate of the isolator is kept fixed, whereas prescribed in-plane displacements are applied to the top surface according to the planned testing protocol.

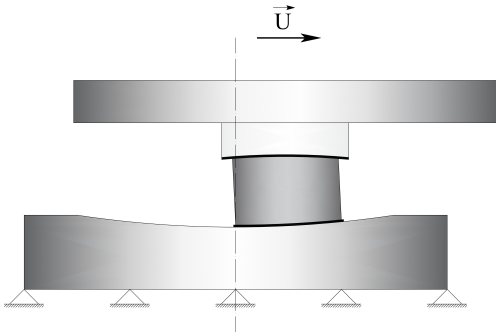

Fig. 2. Scheme of the characterization test

The numerical results describing the interface response in terms of the force-displacement relationships (or U-F relationships) obtained using the testing protocol depicted in Fig. 3, for two orthogonal directions, denoted as X- and Y-, are shown in Fig. 4 and Fig. 5, respectively.

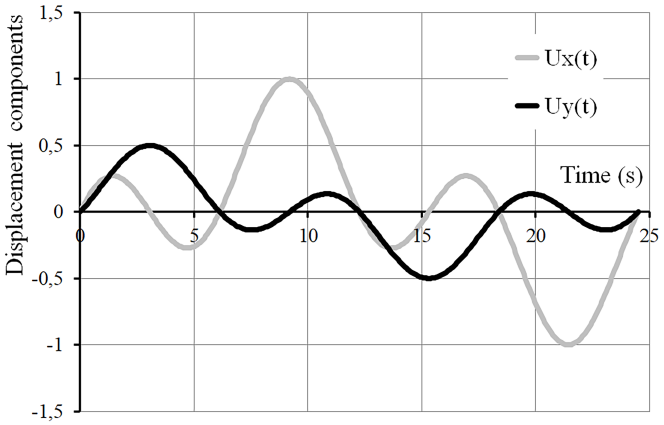

Fig. 3. Testing protocol for displacements

2. Seismic Isolator Considered as a Mechanical System with Three Degrees of Freedom

The slider, taken as a material point, has three degrees of freedom (r, θ, φ). The equations of motion are derived by using the Lagrangian formalism as follows:

$$\frac{d}{dt}\left(\frac{\partial L}{\partial \dot{q}_i}\right) - \frac{\partial L}{\partial q_i} = Q_i, \; L = E_k - E_p. \tag{2}$$

In equation (2), $\dot{q}_i$ denote the generalized velocities, q_i correspond to the generalized coordinates, and Q_i represent the generalized forces $(i = 1, \ldots, 3)$, while E_k and E_p stand

for the kinetic and potential energy, respectively. In the expanded form, a system of three equations is obtained:

$$\begin{cases} -mr(\dot{\theta}^2 + \dot{\varphi}^2 \sin^2(\theta)) - N\cos(\theta) = Q_r, \\ mr^2\ddot{\theta} - mr^2\dot{\varphi}^2 \sin(\theta)\cos(\theta) + Nr\sin(\theta) = Q_\theta, \\ mr^2(\ddot{\varphi}\sin^2(\theta) + 2\dot{\varphi}\dot{\theta}\sin(\theta)\cos(\theta)) = Q_\varphi. \end{cases} \tag{3}$$

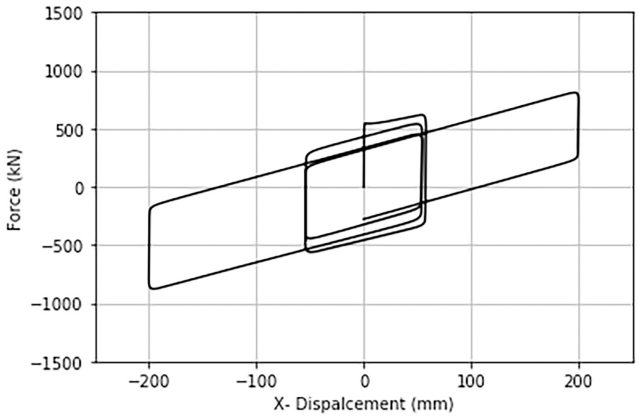

Fig. 4. Force-displacement relationship in the X-direction: $U_x - F_x$

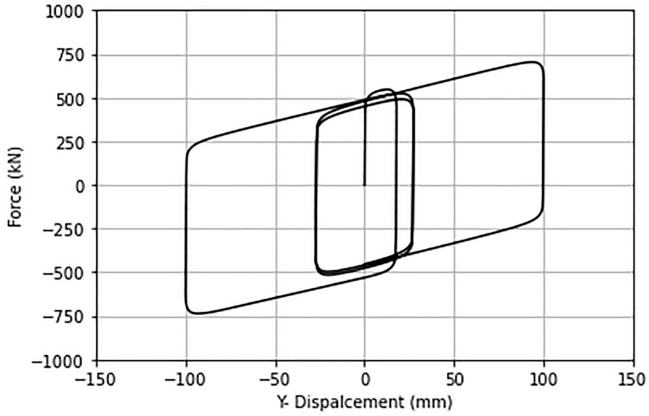

Fig. 5. Force-displacement relationship in the Y-direction: $U_y - F_y$

The generalized forces on the right-hand sides of the equations in the system of equations (3) are obtained by summing the inertia force components with the normal reaction R_n (for the first equation) and the friction forces R_θ and R_φ (for the second and third equations, respectively), as shown in Fig.6:

$$\begin{cases} -mr(\dot{\theta}^2 + \dot{\varphi}^2 \sin^2(\theta)) - N\cos(\theta) = -ma_r - R_n, \\ mr^2\ddot{\theta} - mr^2\dot{\varphi}^2 \sin(\theta)\cos(\theta) + Nr\sin(\theta) = r(-ma_\theta + R_\theta), \\ mr^2(\ddot{\varphi}\sin^2(\theta) + 2\dot{\varphi}\dot{\theta}\sin(\theta)\cos(\theta)) = r\sin(\theta)(-ma_\varphi + R_\varphi). \end{cases} \tag{4}$$

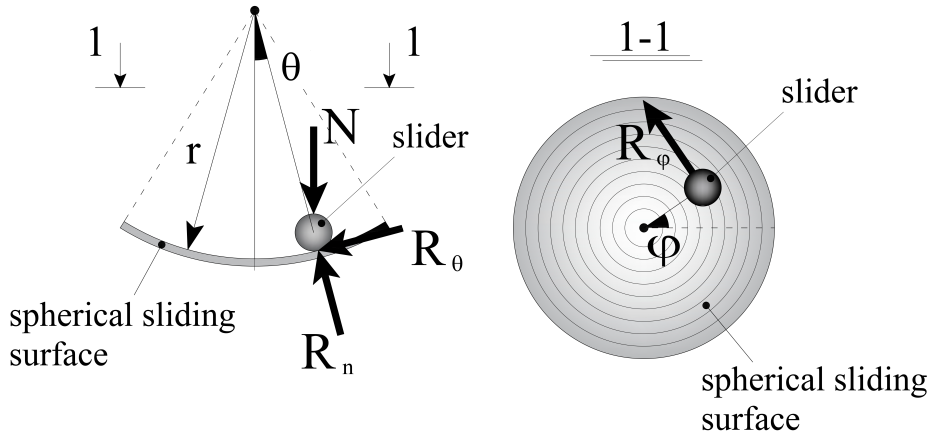

Fig. 6. Generalized coordinates, normal reaction, and friction forces acting on the slider

In equation (4), the acceleration vector is defined in polar coordinates $(a_r,\ a_\theta,\ a_\varphi)$, but the recorded acceleration contains the Cartesian components of the acceleration vector $(a_x,\ a_y,\ a_z)$. The equation below describes the relationship between the acceleration vector components expressed in polar and Cartesian coordinate systems:

$$\begin{bmatrix} a_r \\ a_\theta \\ a_\varphi \end{bmatrix} = \begin{bmatrix} \cos(\varphi)\sin(\theta) & \sin(\varphi)\sin(\theta) & -\cos(\theta) \\ \cos(\varphi)\cos(\theta) & \sin(\varphi)\cos(\theta) & \sin(\theta) \\ -\sin(\varphi) & \cos(\varphi) & 0 \end{bmatrix} \cdot \begin{bmatrix} a_x \\ a_x \\ a_z \end{bmatrix}. \tag{5}$$

Given that the slider is forced to move along the sliding surface, an expression for the normal reaction can be obtained from the first equation in the system of equations (4):

$$R_n = -mr(\dot\theta^2 + \dot\varphi^2\sin^2(\theta)) - mg\cos(\theta) + m(\cos(\varphi)\sin(\theta)a_x + \sin(\varphi)\sin(\theta)a_y - \cos(\theta)a_z). \tag{6}$$

Leveraging the expression for the normal reaction, the friction force components are expressed as:

$$\begin{aligned} R_\theta &= -\mu R_n \mathrm{sgn}(\dot\theta), \\ R_\varphi &= -\mu R_n \mathrm{sgn}(\dot\theta\sin(\theta)). \end{aligned} \tag{7}$$

Thus, the system of equations (4) reduces to the following two equations:

$$\begin{aligned} &\ddot\theta - \mu\dot\theta^2\mathrm{sgn}(\dot\theta) + [g/r - \dot\varphi^2\cos(\theta) + a_z/r - \mu\dot\varphi^2(\sin(\theta)\mathrm{sgn}(\dot\theta) + (\mu/r)(\cos(\varphi)a_x + \\ &+ \sin(\varphi)a_y)\mathrm{sgn}(\dot\theta)]\sin(\theta) + (1/r)(\cos(\varphi)\cos(\theta)a_x + \sin(\varphi)\cos(\theta)a_y) - \\ &- (\mu/r)(g\cos(\theta) + \cos(\theta)a_z)\mathrm{sgn}(\ddot\theta) = 0, \end{aligned} \tag{8}$$

$$\begin{aligned} &\ddot\varphi - \dot\varphi^2\mu\sin(\theta)\mathrm{sgn}(\sin(\theta)\dot\varphi) + 2\dot\varphi\dot\theta\tan(\theta) + (1/r\sin(\theta))(\mu\sin(\theta)a_y\mathrm{sgn}(\sin(\theta)\dot\varphi) - \\ &- a_x)\sin(\varphi) + (1/r\sin(\theta))(\cos(\varphi)a_y - \mu(r\dot\theta^2 + g\cos(\theta) - \cos(\varphi)\sin(\theta)a_x + \\ &+ \cos(\theta)a_z)\mathrm{sgn}(\sin(\theta)\dot\varphi) = 0, \end{aligned} \tag{9}$$

which are solved numerically.

3. Dynamic Response Analysis of a Structure with Seismic Isolation

The general-purpose finite-element code ANSYS Mechanical APDL is employed to build the finite-element model of a reinforced concrete structure (with elasticity modulus $E = 30$ GPa, Poisson's ratio $\nu = 0.2$, and density $\rho = 2500$ kg/m^3) shown in Fig. 7. Point masses ($m = 2000$ kg) are defined at each level, at points E, F, G, H, I, J, K, L, M, N, O, and P. Two versions of the model are developed: one equipped with base isolation and another without seismic isolation, for reference. For the reference model (without seismic isolation), the seismic input is applied to all nodes located at $z = 0$, whereas, for the model of the seismically isolated structure, seismic accelerations act at locations where the friction pendulum bearings are installed (i.e., points A, B, C, and D at $z = 0$, see Fig. 7, b).

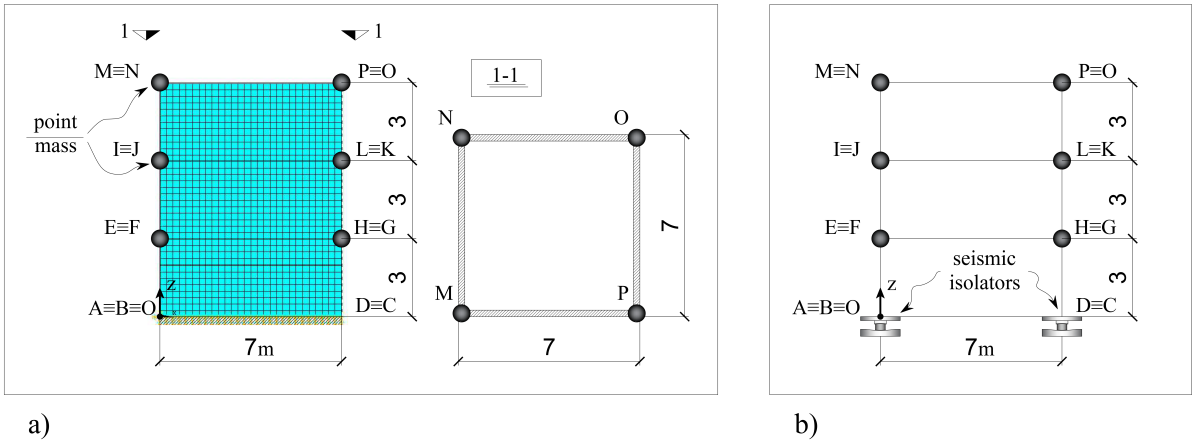

Fig. 7. Reference structure without seismic isolation (a), structure with base isolation (b)

The generated finite-element mesh (Fig. 7, a) contains 4044 finite elements SHELL181 and 12 finite elements MASS21. SHELL181 is a four-node element with six degrees of freedom per node (translations in the X-, Y-, and Z-directions and rotations about the X-, Y-, and Z-axes). MASS21 is a point element with six degrees of freedom (translations in the nodal X-, Y-, and Z- directions and rotations about the nodal X-, Y-, and Z-axes).

A transient analysis is then carried out using the recorded acceleration time series (the X-component of the input is displayed in Fig. 8). It should be noted that the employed input is an excitation with the X-, Y-, and Z- components.

The response of the structure is obtained in terms of displacement evolution (Fig. 9) and acceleration evolution (Fig. 10) monitored at point P, as shown in Fig. 7.

It is apparent that the implementation of friction pendulum seismic isolators leads to a significant decrease in the monitored displacement. The decrease in acceleration is not so well pronounced. In this context, seismic isolation can positively modify the fragility curves (or surfaces) typically employed in quantitative risk assessment.

A comparison of the dynamic response of the base-isolated structure for various characteristics of the friction pendulum bearing R and μ is given in Fig. 11. An increase in the equivalent radius of curvature (from 3 m to 4 m) leads to a decrease in the maximum value of the monitored displacement up to 33 %. On the other hand, an (almost) double increase in the friction coefficient increases the maximum absolute value of the monitored displacement by 49 %. It should be noted that choosing the equivalent radius of curvature is much easier to

control, given that the friction coefficient is strongly material specific. However, an in-depth understanding of the interface behavior (i.e., the precise assessment of the friction coefficient degradation) is crucial for accurately predicting the response of the isolator and the base-isolated structure.

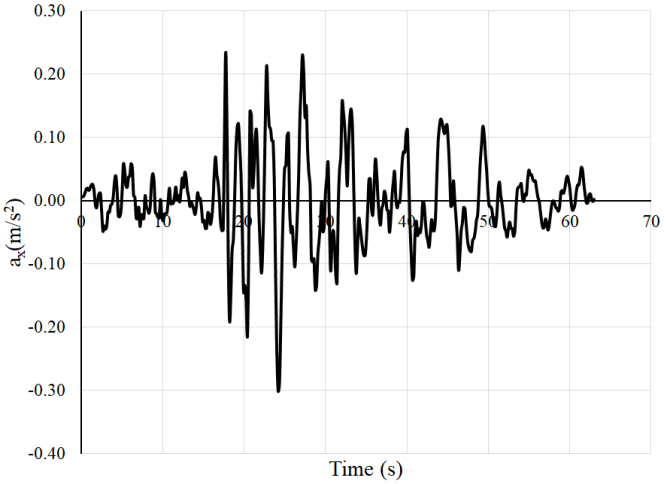

Fig. 8. X-component of the input acceleration time series

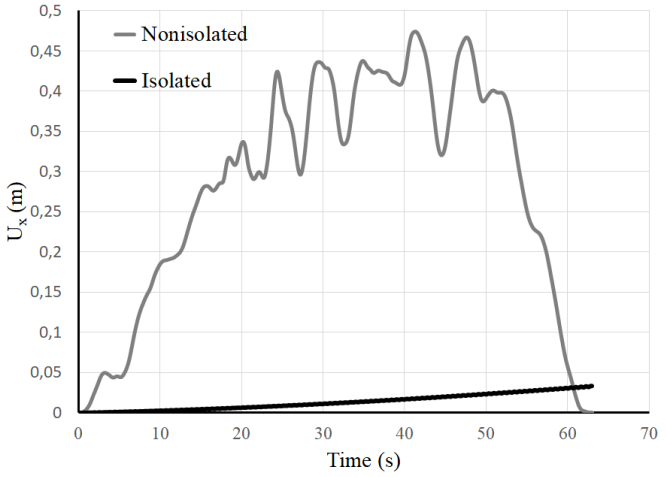

Fig. 9. Comparison of the X-component of the displacement at point P for the nonisolated and isolated structures

It should be mentioned that the numerical results are obtained by assuming a constant value for the friction coefficient. As an illustration of a variable friction coefficient, its evolution (and, more precisely, its decrease in the X-direction), predicted in the context of the characterization test (Fig. 2), is shown in Fig. 12.

These results are consistent with the data provided in [29], on a decrease in the friction coefficient from 0.07 to 0.04.

In a comprehensive research with an experimental basis, reported in [6], it was deduced that the friction coefficient depends on the sliding velocity and the normal pressure acting on the sliding surface. The behavior illustrated in Fig. 12 has been obtained [30]

using phenomenological models that postulate a dependence of the friction coefficient on the sliding velocity, normal pressure, and the rise in temperature during sliding [31, 32]. The temperature rise can be experimentally detected using either thermocouples [33, 34] or thin-film thermocouples [35]. The accurate assessment of available models reveals discrepancies between theoretical predictions and experimental data, which can reach up to 40–50 % for sliding paths longer than 10 m. The above implies that simulation of the characterization test may and should be included in the design of bearings for a better model constant identification prior to the time history analysis of the base-isolated structure.

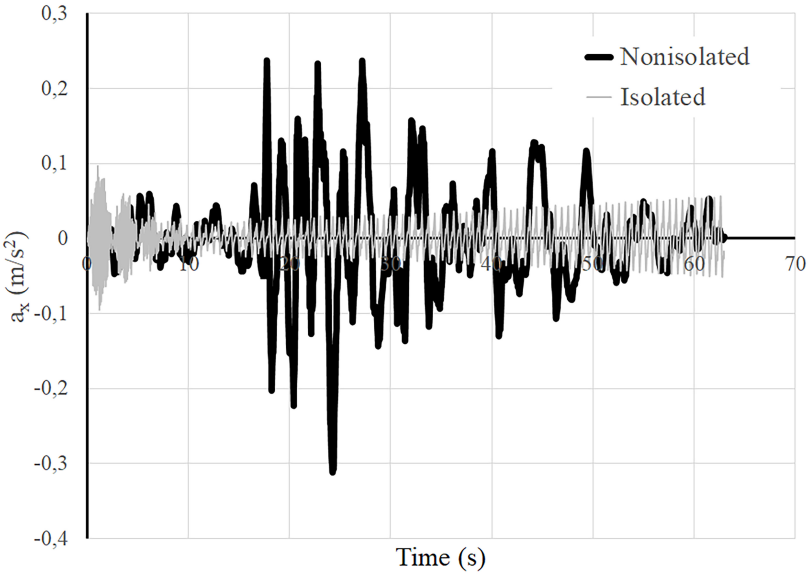

Fig. 10. Comparison of the X-component of the acceleration at point P for the nonisolated and isolated structures

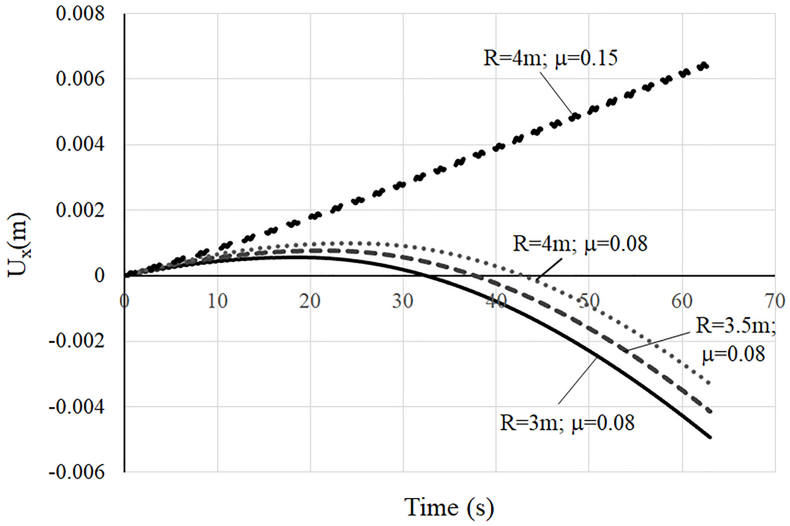

Fig. 11. Comparison of the X-component of the displacement at point P for various characteristics of the friction pendulum bearing

Conclusions

Some theoretical models of friction pendulum seismic isolators, their applications in the mathematical modeling of experimental characterization of bearings (such as the U-F relationships), and their implementation in the analysis of the dynamic response of a structure equipped with friction pendulum isolators were considered. Although SDOF models possess some drawbacks in predicting the friction pendulum bearing within base-isolated structures, they should be employed in the model constant identification phase. Models that consider all degrees of freedom for the isolator provide a more accurate assessment of its multiaxial response and are better suited for the analysis of the dynamic behavior of the overall structure. Additionally, lightweight analytical models are clearly more efficient in a transient finite-element analysis compared to detailed high-fidelity finite-element models of the bearings.

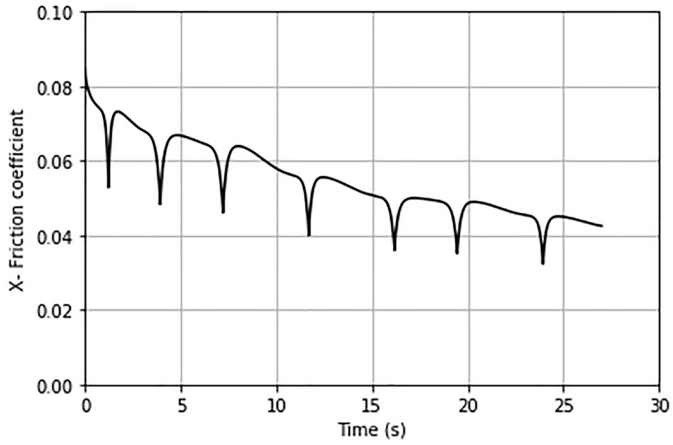

Fig. 12. Change in the friction coefficient, in the X-direction, obtained in a simulation of a friction pendulum bearing characterization test

The obtained numerical results showcase the favorable effect of seismic isolation on the dynamic response of a structure during earthquakes. The proposed algorithm can be applied for the design of seismic isolators, for their placement within the structure, as well as for optimizing the response of the structure considering a specific seismic hazard. In some cases, base isolation positively modifies the fragility curves/surfaces of the structure, providing a less conservative risk assessment for structures in seismic regions.

Conflicts of Interest. The author declares no conflicts of interest.

Конфликт интересов. Автор заявляет об отсутствии конфликта интересов.

References

1. Kavyashree B.G., Patil S., Rao V.S. Review on vibration control in tall buildings: From the perspective of devices and applications. *Int. J. Dyn. Control*, 2021, vol. 9, no. 3, pp. 1316–1331. https://doi.org/10.1007/s40435-020-00728-6.

2. Naeim F., Kelly J.M. *Design of Seismic Isolated Structures: From Theory to Practice*. New York, NY, John Wiley & Sons, 1999. xiv, 290 p. https://doi.org/10.1002/9780470172742.

3. Zayas V.A., Low S.S., Mahin S.A. A simple pendulum technique for achieving seismic isolation. *Earthquake Spectra*, 1990, vol. 6, no. 2, pp. 317–333. https://doi.org/10.1193/1.1585573.

4. Megget L.M. Analysis and design of a base-isolated reinforced concrete frame building. *N. Z. Soc. Earthquake Eng.*, 1978, vol. 11, no. 4, pp. 245–254. https://doi.org/10.5459/bnzsee.11.4.245-254.

5. Mokha A., Constantinou M., Reinhorn A. Teflon bearings in base isolation. I: Testing. *J. Struct. Eng.*, 1990, vol. 116, no. 2, pp. 438–454. https://doi.org/10.1061/(ASCE)0733-9445(1990)116:2(438).

6. Constantinou M.C., Mokha A., Reinhorn A. Teflon bearings in base isolation. II: Modeling. *J. Struct. Eng.*, 1990, vol. 116, no. 2, pp. 455–474. https://doi.org/10.1061/(ASCE)0733-9445(1990)116:2(455).

7. Mokha A., Constantinou M.C., Reinhorn A.M. Further results on frictional properties of Teflon bearings. *J. Struct. Eng.*, 1991, vol. 117, no. 2, pp. 622–626. https://doi.org/10.1061/(ASCE)0733-9445(1991)117:2(622).

8. Mokha A., Amin N., Constantinou M.C., Zayas V. Seismic isolation retrofit of large historical building. *J. Struct. Eng.*, 1996, vol. 122, no. 3, pp. 298–308. https://doi.org/10.1061/(ASCE)0733-9445(1996)122:3(298).

9. Kim H.-m., Constantinou M.C. Performance-based testing specifications for seismic isolators. *Earthquake Eng. Struct. Dyn.*, 2023, vol. 52, no. 15, pp. 5141–5161. https://doi.org/10.1002/eqe.4006.

10. Castaldo P., Palazzo B., Della Vecchia P. Seismic reliability of base-isolated structures with friction pendulum bearings. *Eng. Struct.*, 2015, vol. 95, pp. 80–93. https://doi.org/10.1016/j.engstruct.2015.03.053.

11. Tsopelas P., Constantinou M.C., Kim Y.S., Okamoto S. Experimental study of FPS system in bridge seismic isolation. *Earthquake Eng. Struct. Dyn.*, 1996, vol. 25, no. 1, pp. 65–78. https://doi.org/10.1002/(SICI)1096-9845(199601)25:1%3C65::AID-EQE536%3E3.0.CO;2-A.

12. Fenz D.M., Constantinou M.C. Spherical sliding isolation bearings with adaptive behavior: Theory. *Earthquake Eng. Struct. Dyn.*, 2008, vol. 37, no. 2, pp. 163–183. https://doi.org/10.1002/eqe.751.

13. Fenz D.M., Constantinou M.C. Spherical sliding isolation bearings with adaptive behavior: Experimental verification. *Earthquake Eng. Struct. Dyn.*, 2008, vol. 37, no. 2, pp. 185–205. https://doi.org/10.1002/eqe.750.

14. Lee D., Constantinou M.C. Quintuple friction pendulum isolator: Behavior, modeling, and validation. *Earthquake Spectra*, 2016, vol. 32, no. 3, pp. 1607–1626. https://doi.org/10.1193/040615EQS053M.

15. Zheng W., Tan P., Li J., Wang H., Liu Y. Superelastic pendulum isolator with multi-stage variable curvature for seismic resilience enhancement of cold-regional bridges. *Eng. Struct.*, 2023, vol. 284, art. 115960. https://doi.org/10.1016/j.engstruct.2023.115960.

16. Admane H.A., Murnal P. Comparative analysis of SIVC systems using simplified analytical modeling for practical design. *Pract. Period. Struct. Des. Constr.*, 2021, vol. 26, no. 1, art. 04020051. https://doi.org/10.1061/(ASCE)SC.1943-5576.0000536.

17. Zhang F., Deng J., Cao S., Dang X. Experimental and simulation studies of adaptive stiffness double friction pendulum bearing. *Structures*, 2023, vol. 57, art. 105026. https:// doi.org/10.1016/j.istruc.2023.105026.

18. Shahbazi P., Taghikhany T. Sensitivity analysis of variable curvature friction pendulum isolator under near-fault ground motions. *Smart Struct. Syst.*, 2017, vol. 20, no. 1, pp. 23–33. https://doi.org/10.12989/sss.2017.20.1.023.

19. Shaikhzadeh A.A., Karamoddin A. Effectiveness of sliding isolators with variable curvature in near-fault ground motions. *The Struct. Des. Tall Spec. Build.*, 2016, vol. 25, no. 6, pp. 278–296. https://doi.org/10.1002/tal.1258.

20. Zhang C., Duan C., Sun L. Inter-storey isolation versus base isolation using friction pendulum systems. *Int. J. Struct. Stab. Dyn.*, 2024, vol. 24, no. 2, art. 2450022. https://doi.org/10.1142/S0219455424500226.

21. Almazán J.L., De La Llera J.C., Inaudi J.A. Modeling aspects of structures isolated with the friction pendulum system. *Earthquake Eng. Struct. Dyn.*, 1998, vol. 27, no. 8, pp. 845–867. https://doi.org/10.1002/(SICI)1096-9845(199808)27:8<845::AID-EQE760>3.0.CO;2-T.

22. Mosqueda G., Whittaker A.S., Fenves G.L.Characterization and modeling of friction pendulum bearings subjected to multiple components of excitation. *J. Struct. Eng.*, 2004, vol. 130, no. 3, pp. 433–442. https://doi.org/10.1061/(ASCE)0733-9445(2004)130:3(433).

23. Wang Y.-P., Chung L.-L., Liao W.-H. Seismic response analysis of bridges isolated with friction pendulum bearings. *Earthquake Eng. Struct. Dyn.*, 1998, vol. 27, no. 10, pp. 1069–1093. https://doi.org/10.1002/(SICI)1096-9845(199810)27:10<1069::AID-EQE770>3.0.CO;2-S.

24. Tsai C.S., Chiang T.-C., Chen B.-J. Finite element formulations and theoretical study for variable curvature friction pendulum system. *Eng. Struct.*, 2003, vol. 25, no. 14, pp. 1719–1730. https://doi.org/10.1016/S0141-0296(03)00151-2.

25. Monti G., Petrone F. Analytical thermo-mechanics 3D model of friction pendulum bearings. *Earthquake Eng. Struct. Dyn.*, 2016, vol. 45, no. 6, pp. 957–977. https://doi.org/10.1002/eqe.2693.

26. Asteris P.G., Nozhati S., Nikoo M., Cavaleri L., Nikoo M. Krill herd algorithm-based neural network in structural seismic reliability evaluation. *Mech. Adv. Mater. Struct.*, 2019, vol. 26, no. 13, pp. 1146–1153. https://doi.org/10.1080/15376494.2018.1430874.

27. Mekaoui N., Saito T. A deep learning-based integration method for hybrid seismic analysis of building structures: Numerical validation. *Appl. Sci.*, 2022, vol. 12, no. 7, art. 3266. https://doi.org/10.3390/app12073266.

28. Yavas M.S., Gao Z., Mekaoui N., Saito T. A machine learning-based hybrid seismic analysis of a lead rubber bearing isolated building specimen. *Soil Dyn. Earthquake Eng.*, 2023, vol. 174, art. 108217. https://doi.org/10.1016/j.soildyn.2023.108217.

29. Li J., Kishiki S., Yamada S., Yamazaki S., Watanabe A., Terashima M. Energy-based prediction of the displacement of DCFP bearings. *Appl. Sci.*, 2020, vol. 10, no. 15, art. 5259. https://doi.org/10.3390/app10155259.

30. Zhelyazov T., Debray K. Prediction of the thermo-mechanical behavior of a sliding isolator based on finite element and analytical analysis. *Proc. 2020 III Int. Con. on High Technology for Sustainable Development (HiTech)*. Sofia, IEEE, 2020, pp. 1–6. https://doi.org/10.1109/HiTech51434.2020.9363973.

31. Lomiento G., Bonessio N., Benzoni G. Friction model for sliding bearings under seismic excitation *J. Earthquake Eng.*, 2013, vol. 17, no. 8, pp. 1162–1191. https://doi.org/10.1080/13632469.2013.814611.

32. Kumar M., Whittaker A.S., Constantinou M.C. Characterizing friction in sliding isolation bearings. *Eng. Struct. Dyn.*, 2015, vol. 44, no. 9, pp. 1409–1425. https://doi.org/10.1002/eqe.2524.

33. Quaglini V., Bocciarelli M., Gandelli E., Dubini P. Numerical assessment of frictional heating in sliding bearings for seismic isolation. *J. Earthquake Eng.*, 2014, vol. 18, no. 8, pp. 1198–1216. https://doi.org/10.1080/13632469.2014.924890.

34. De Domenico D., Ricciardi G., Benzoni G. Analytical and finite element investigation on the thermo-mechanical coupled response of friction isolators under bidirectional excitation. *Soil Dyn. Earthquake Eng.*, 2018, vol. 106, pp. 131–147. https://doi.org/10.1016/j.soildyn.2017.12.019.

35. Li J., Yang K., Xiang Y., Tan P. Experimental investigation of frictional heating in variable friction pendulum bearings using thin-film thermocouples. *Tribol. Int.*, 2025, vol. 212, art. 110982. https://doi.org/10.1016/j.triboint.2025.110982.

Author Information

Todor Zhelyazov, PhD, Researcher, National Institute of Geophysics, Geodesy and Geography (NIGGG), Bulgarian Academy of Sciences

E-mail: *elovar@yahoo.com*

ORCID: https://orcid.org/0009-0001-1889-3789

Информация об авторах

Тодор Желязов, PhD, научный сотрудник, Национальный институт геофизики, геодезии и географии (НИГГГ), Болгарская академия наук

E-mail: *elovar@yahoo.com*

ORCID: https://orcid.org/0009-0001-1889-3789

Received August 16, 2025
Accepted October 6, 2025

Поступила в редакцию 16.08.2025
Принята к публикации 6.10.2025